Astron. Astrophys. 349, L9–L12 (1999)

ASTRONOMY AND ASTROPHYSICS

LETTER

Letter to the Editor

The broad-band spectrum of OAO1657–415 with *BeppoSAX*: in search of cyclotron lines

M. Orlandini[1], D. Dal Fiume[1], S. Del Sordo[2], F. Frontera[1,3], A.N. Parmar[4], A. Santangelo[2], and A. Segreto[2]

[1] Istituto Tecnologie e Studio Radiazioni Extraterrestri, TeSRE/CNR, via Gobetti 101, I-40129 Bologna, Italy
[2] Istituto Fisica Cosmica e Applicazioni all'Informatica, IFCAI/CNR, via La Malfa 153, I-90146 Palermo, Italy
[3] Università di Ferrara, Dipartimento di Fisica, via Paradiso 11, I-44100 Ferrara, Italy
[4] Astrophysics Division, Space Science Department of ESA, ESTEC, 2200 AG Noordwijk, The Netherlands

Received 8 June 1999 / Accepted 9 August 1999

Abstract. We report on a 30 ks observation of the high-mass X–ray binary pulsar OAO1657–415 performed by *BeppoSAX* on September 1998. The wide band spectrum is well fit by both a cutoff power law, or a power law modified by a high energy cutoff, plus a fluorescence Iron line at 6.5 keV. The two models are statistically equivalent. The inclusion of a cyclotron resonance feature at ∼36 keV – corresponding to a magnetic field strength $3.2\,(1+z)\times10^{12}$ G, where z is the gravitational redshift – improves significantly the χ^2 for the cutoff model but only marginally for the power law plus high energy cutoff model. The statistical significance of our data is not adequate to discriminate between the two models, and even the *Normalized Crab Ratio* technique, successfully used to pinpoint cyclotron features in the spectra of other X–ray pulsars, is not conclusive in answering the question whether the feature is real or it is an artifact due to an improper modeling of the continuum used to fit the data.

Key words: magnetic fields – stars: binaries: close – stars: neutron – stars: pulsars: individual: OAO1657–415 – X-rays: stars

1. Introduction

X–ray binary pulsars (XRBs) display a common signature in their X–ray spectra: the presence of a high-energy cutoff that makes their spectra rapidly drop above ∼40–50 keV. There are only few exceptions to this general behaviour, and OAO1657–415 is one of them: indeed, this source displays one of the hardest X–ray spectra amongst XRBs, with no steepening up to 100 keV (Byrne et al. 1981). In those cases in which cyclotron line features are observed, the cutoff energy $E_{\rm c}$ seems to be related to the cyclotron line energy $E_{\rm cyc}$ through a phenomenological relation found by Makishima & Mihara (1992): $E_{\rm cyc}\simeq(1.2\text{–}2.5)\cdot E_{\rm c}$. Because $E_{\rm cyc}$ is related to the neutron star magnetic field strength B_{12} in units of 10^{12} G by the relation $E_{\rm cyc}=11.6\,B_{12}\,(1+z)^{-1}$ G, where z is the gravitational redshift, a measurement of $E_{\rm c}$ can give an estimate of the neutron star magnetic field. For OAO1657–415 we therefore expect $B_{12}\gtrsim10$: only another XRB, A0535+26, is known to possess such a strong magnetic field (Grove et al. 1995).

OAO1657–415 was discovered by the *Copernicus* satellite (Polidan et al. 1978), and soon after its discovery a 38 s pulsation was detected by the A2 experiment aboard *HEAO 1* (White & Pravdo 1979). The optical counterpart of OAO1657–415 was first identified with the spectroscopic binary V861 Sco, but subsequent observations (Armstrong et al. 1980; Parmar et al. 1980) produced positional error boxes that excluded this star as the optical counterpart that is, up today, still unknown. Since 1991 OAO1657–415 has been monitored continuously by the BATSE experiment aboard *CGRO*. This allowed the discovery of X–ray eclipses by the stellar companion and the determination of a 10.44 d orbital period (Chakrabarty et al. 1993). The distance to the source is not known, but a lower limit of 11 kpc has been determined by assuming that the neutron star is rotating at its equilibrium period. Because of its low galactic latitude, the low energy (≲2 keV) spectrum of OAO1657–415 is very absorbed, with $\rm N_H\gtrsim10^{23}$ cm^{-2}. *GINGA* observations of the source revealed the presence of a soft excess, below 3 keV, modeled with a 0.3 keV blackbody (Kamata et al. 1990). The OAO1657–415 X–ray spectrum also displays a fluorescence Iron line at ∼6.6 keV (White & Pravdo 1979; Kamata et al. 1990).

2. X–ray observation and data analysis

OAO1657–415 was observed by the Narrow Field Instruments (NFIs) aboard the Italian-Dutch X–ray satellite *BeppoSAX* (Boella et al. 1997a) from 1998 September 4 15:41:46 to September 5 07:20:35 UT. All the NFIs performed nominally during the observation, namely the two imaging instruments LECS (0.1–10 keV; Parmar et al. 1997) and MECS (1.5–10 keV; Boella et al. 1997b), and the two mechanically collimated instruments HPGSPC (4–180 keV; Manzo et al. 1997)

Send offprint requests to: orlandini@tesre.bo.cnr.it

Table 1. Best fit parameters for the two models that fit the OAO1657–415 continuum: a cutoff power law and a power law plus high energy cutoff. For both the models we show the best fit parameters without the cyclotron resonance feature (CRF) and with it. Because the CRF width is not well constrained by the fit, we present also the best-fit parameters for a CRF width fixed at 10 keV

Parameter	Value[a]				
	Cutoff			Power Law + Highcut	
	w/o CRF	w/ CRF	w/ CRF	w/o CRF	w/ CRF
N_H (10^{22} cm^{-2})	12.1 ± 0.4	12.0 ± 0.4	12.1 ± 0.4	$12.7^{+0.4}_{-0.2}$	$12.7^{+0.3}_{-0.4}$
α	0.41 ± 0.04	$0.44^{+0.11}_{-0.06}$	0.43 ± 0.04	0.83 ± 0.04	$0.83^{+0.03}_{-0.06}$
E_c (keV)	16.4 ± 0.5	19^{+18}_{-2}	17.5 ± 0.7	$13.0^{+0.5}_{-0.4}$	$12.9^{+0.5}_{-0.4}$
E_f (keV)				$21.2^{+0.6}_{-0.4}$	$22.2^{+0.8}_{-0.7}$
E_{Fe} (keV)	6.48 ± 0.04	6.48 ± 0.04	6.48 ± 0.04	6.47 ± 0.04	6.47 ± 0.04
σ_{Fe} (keV)	$0.33^{+0.08}_{-0.07}$	$0.35^{+0.08}_{-0.07}$	$0.34^{+0.08}_{-0.07}$	0.42 ± 0.05	$0.42^{+0.05}_{-0.06}$
E_{CRF} (keV)		30^{+7}_{-25}	36 ± 3		44^{+11}_{-5}
τ_{CRF}		$0.18^{+0.09}_{-0.13}$	0.12 ± 0.05		$0.11^{+0.06}_{-0.04}$
W_{CRF} (keV)		28^{+26}_{-15}	10 (fixed)		11^{+19}_{-7}
χ^2_ν (dof)	1.129 (572)	1.088 (569)	1.094 (570)	1.127 (571)	1.117 (568)

[a] Uncertainties at 90% confidence for a single parameter

and PDS (15–200 keV; Frontera et al. 1997). Data were collected in direct mode, providing information on time, energy, and position. Good data were selected using default criteria. The net exposure times for the four NFIs were 9.2, 26, 11.7, and 10.8 ks for the LECS, MECS, HPGSPC, and PDS, respectively. These differences are due to the constraint that the LECS must operate in satellite night time, and rocking of the collimated NFIs. For the imaging NFIs data were extracted from $4'$ circular regions centered on the source position.

The background for the imaging NFIs was estimated from standard background blank field measurements. Because of its low galactic latitude, and therefore possible contamination by background sources, we also extracted spectra from two blank $4'$ circular regions offset by $11'$ with respect to the source. Our result on the spectral analysis does not depend on which background was used: for example, the 6–7 keV MECS count rate in the offset backgrounds is less than 1% of the source count rate in the same band. For the non-imaging NFIs the background was monitored by rocking the collimators off-source by 3° for HPGSPC (one-side rocking), and $3.^\circ5$ for PDS (two-side rocking). The off-source fields were checked for the presence of contaminating sources: one of the PDS background fields was found to show an excess count rate with respect to the other, a clear signature of contaminating sources, and therefore was not used for the estimation of the source background.

The contribution of the Galactic Ridge (GR) emission was estimated by using the results from *RXTE* observations of the galactic plane (Valinia & Marshall 1998). We found that the ratio between the GR and the source flux is always $\lesssim 10^{-3}$, therefore we exclude any contribution of the GR emission to our spectral data.

The spectra of each *BeppoSAX* NFI were first fit separately to derive the best model able to describe the broad band spectrum. We find that the LECS and MECS spectra can be described in terms of an absorbed power law plus a Gaussian line in emission, while the PDS spectrum clearly presents a deviation from a pure power law, with a steepening above $\sim$20 keV. We therefore used a power law, modified at low energy by photoelectrical absorption and at high energy by a cutoff, to describe the broad band spectrum. Variable normalizations among the NFIs, found in agreement with those obtained from the fit to the Crab spectrum, were introduced to take into account known calibration uncertainties. Both an exponential cutoff (EC) and a high-energy cutoff (HEC; White et al. 1983) yield a good fit, while a thermal bremsstrahlung did not fit our data. Also the smoother Fermi-Dirac cutoff (Tanaka 1986) did not adequately describe the high energy tail. An F-test shows that the probability of chance improvement (PCI) of the χ^2 between the EC and HEC models is 78%, therefore they are statistically equivalent. In Table 1 we present the best-fit parameters for both the two models.

Concerning the low ($\lesssim$3 keV) energy part of the spectrum, our data do not show any soft excess as observed by *GINGA* (Kamata et al. 1990). The Iron line equivalent width is 360 ± 280 eV, in agreement with the *GINGA* result but lower than the *HEAO 1* measurement (White & Pravdo 1979). This confirms the possible contamination by the GR emission of the latter, as discussed by Kamata et al. (1990). The Iron line energy found by *BeppoSAX* is lower than that measured by *GINGA* (6.60 ± 0.08 keV) and *HEAO 1* (6.7 ± 0.1 keV). The unabsorbed fluxes in the bands 2–10 and 10–100 keV are 4.7×10^{-10}, and 1.8×10^{-9} erg cm^{-2} s^{-1}, respectively. The total 0.1–100 keV X-ray luminosity is 2.5×10^{35} erg s^{-1} d^2_{kpc}, where d_{kpc} is the OAO1657–415 distance in kpc.

From the form of the residuals above 20 keV we were led to add an extra component to our spectral model, that we interpret in terms of a cyclotron resonance feature (CRF). Both a Lorenzian (Mihara 1995) and a Gaussian in absorption (Soong et al. 1990) improved the fit, and here we will present results obtained with the Lorenzian form of the CRF. The inclusion of the extra component have different significance for the two continuum models. Indeed, an F-test shows that the inclu-

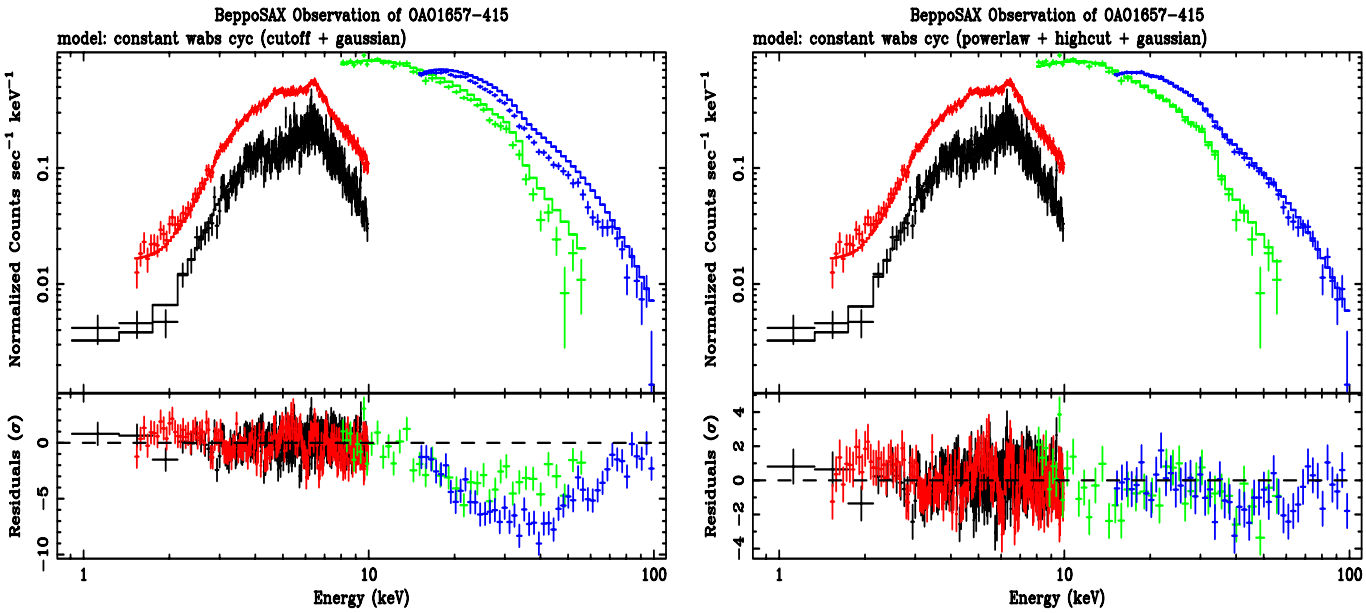

Fig. 1. OAO1657–415 count rate spectrum *(plus signs)* and best-fit continuum model *(histogram)*, together with the fit residuals. On the left the EC model was used, on the right the HEC model. The CRF normalization has been set to zero, in order to show its profile in the residual panel

sion of the CRF improves significantly the χ^2 for the EC model (the PCI is 2.8×10^{-5}), while the PCI for the HEC model is higher (1.1×10^{-2}). In Table 1 we show the best-fit parameters of the CRF, and in Fig. 1 we show both the EC and HEC best-fit spectral models, with the residual CRF Lorenzian line profile shown in the residual panel, obtained by setting the line normalization to zero. We can see very well how the line is significant and very broad by using the EC model, and with much less significance with the HEC model. Because the line width is not well constrained by the fit, we also present in Table 1 the best-fit parameters obtained by fixing the CRF width at 10 keV.

In order to check if the CRF is real or an artifact due to an improper modeling of the continuum, we calculated the ratio between the HPGSPC and PDS count rate spectra with the Crab pulsar count spectrum. This ratio has the advantage of minimizing calibration uncertainties. In Fig. 2, top panel, we can see that this ratio does not show any evident change of slope, as observed in other pulsars (see e.g. Orlandini et al. 1998b; Dal Fiume et al. 1998). By multiplying the Crab ratio by the functional form of the Crab spectrum (Fig. 2, second panel), *i.e.* a power law of index 2.1, and diving by the functional form of the continuum (Fig. 2, third and fourth panels), as obtained from our spectral fits, we are able to emphasize any deviations from the continuum. This *Normalized Crab Ratio* technique has been successfully used to pinpoint CRFs in the spectra of other X–ray pulsars (Dal Fiume et al. 1999). The third panel of Fig. 2 shows a broad line, modeled with a Gaussian line centered at 43^{+18}_{-5} keV and $\sigma_{\rm cyc} = 28^{+17}_{-6}$ keV ($\chi^2/{\rm dof} = 17.7/30$).

The narrow feature at ∼60 keV present in the PDS Crab ratio has $\sigma = 5^{+5}_{-2}$ keV if modeled with a Gaussian in 53–70 keV ($\chi^2/{\rm dof} = 0.18/4$). This value is marginally comparable with the PDS energy resolution of 8.6 keV (FWHM; Frontera et al. 1997) at 62^{+3}_{-2} keV. The inclusion of this feature in the broad-band fit yields a $\chi^2/{\rm dof}$ of 618.19/567. An F-test shows that the PCI of the χ^2 is 17.5%. For these reasons we do not consider it as a real feature.

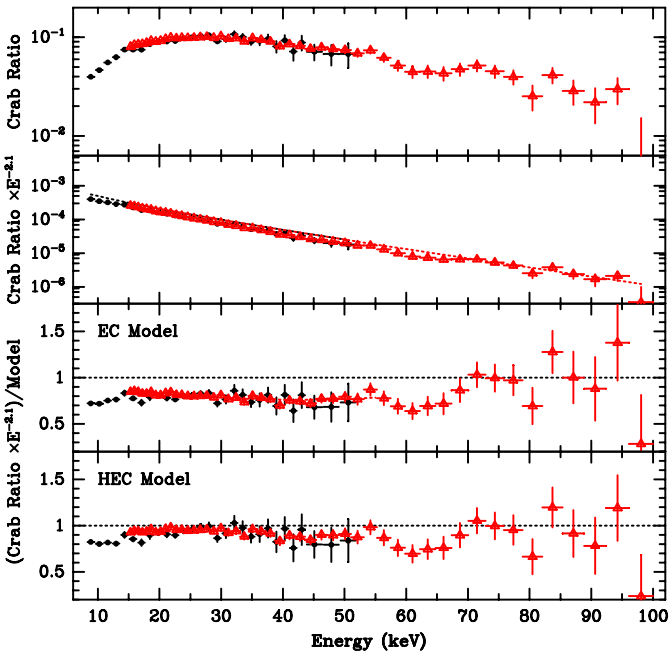

Fig. 2. OAO1657–415 Normalized Crab Ratio. *Top:* Ratio between the HPGSPC *(black dots)* and PDS *(grey triangles)* count rate spectra with the Crab pulsar one. *Second Panel*: Crab ratio multiplied by the functional form of the Crab spectrum, a featureless power law of spectral index 2.1. *Third Panel*: Crab ratio times $E^{-2.1}$ divided by the EC continuum. *Fourth Panel*: The same as the third panel but divided by the HEC continuum

3. Discussion

The main result obtained from the *BeppoSAX* observation of OAO1657–415 is the clear detection of a steepening of the spectrum above 20 keV, and that this drop occurs in two steps. Indeed *BeppoSAX* observations of XRBs have shown that there are actually *two* changes of slope in the high (E$\gtrsim$10 keV) energy part of their spectra: a first change of slope occurs in the $\sim$10–20 keV range, while a second steepening occurs for higher energies. This is partly expressed in the form of the high-energy cutoff (White et al. 1983), that has been used to empirically describe the two-step spectral drop in these sources. In the XRB Vela X–1, for example, the first change of slope occurs at $\sim$24 keV and it can be misinterpreted as a CRF (Orlandini et al. 1998a). For OAO1657–415 we think we are observing the same phenomenon: the high energy part of the spectrum presents two changes of slope: if we model the continuum with only one steepening, then the fit requires the presence of a second one, that can be modeled with a CRF. On the other hand, if we model the continuum with a two-step change of slope (the HEC model) then an additional CRF is not required to describe the spectral drop. The fact that we observe a broad CRF is due to the fact that the OAO1657–415 spectrum is very hard, therefore the steepening is smooth. On the other hand, in the case of a softer spectrum, like in Vela X–1, the steepening is much more abrupt, and therefore the *false* CRF is narrower.

Lacking a model of the continuum able to describe this behaviour, the only way to discriminate a real CRF from an artifact due to an improper modeling of the continuum is through the Crab ratio, which is model independent. In Fig. 3 we show the Normalized Crab Ratios from PDS data obtained for a sample of XRBs observed by *BeppoSAX*. A comparison with Fig. 2 clearly shows that the OAO1657–415 Crab ratio does not pinpoint the CRF as it does for all the other XRBs. The fact that $E_{\rm cyc}$ depends on the adopted continuum seems to rule against a *real* CRF, but it is intriguing that the Makishima & Mihara relation is satisfied for the OAO1657–415 CRF. Furthermore, the relation between $E_{\rm cyc}$ and its FWHM, clearly shown in Fig. 3 where the CRF width increases as $E_{\rm cyc}$ increases, and explained in terms of Doppler broadening of the electrons responsible for the resonance (Mészáros 1992) is fulfilled if we assume for the CRF width a value of 10 keV, which is the one obtained from the HEC fit, and can be considered as a lower limit for the width. In this case the OAO1657–415 surface magnetic field strength would be $(3.1 \pm 0.2) \times 10^{12}\,(1+z)$ G. On the other hands, this relation would not be satisfied by the broader CRF. Pulse phase spectroscopy should be able to resolve this ambiguity. However, longer observations may be needed.

Acknowledgements. This research is supported in part by the Italian Space Agency.

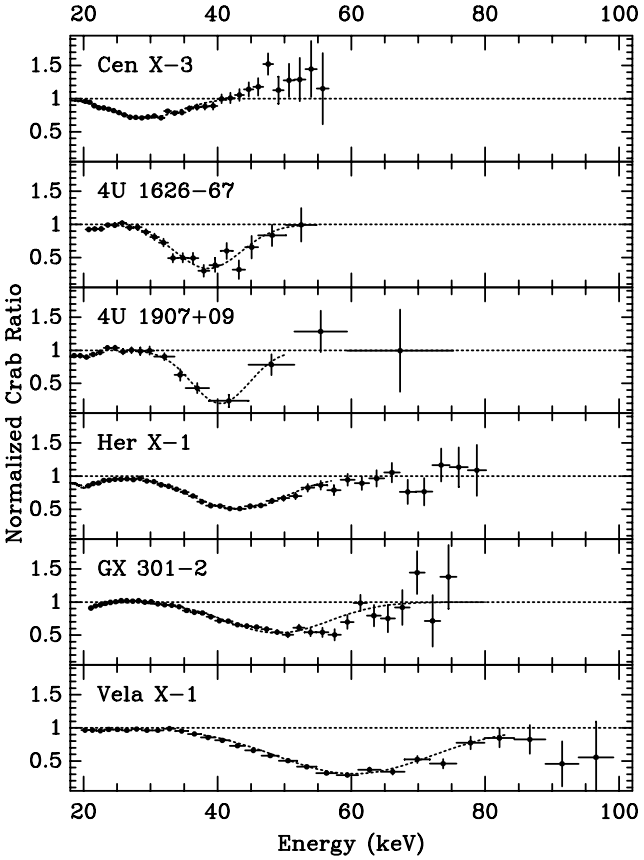

Fig. 3. Normalized Crab Ratios from PDS data obtained for a sample of XRBs observed by *BeppoSAX* (see e.g. Dal Fiume et al. 1999). The continuum drop is modeled with a HEC for all the sources but Cen X–3, for which an EC model is used

References

Armstrong J.T., Johnston M., Bradt H.V., et al., 1980, ApJ, 236, L131
Boella G., Butler R.C., Perola G.C., et al., 1997a, A&AS, 122, 299
Boella G., Chiappetti L., Conti G., et al., 1997b, A&AS, 122, 327
Byrne P.F., Levine A.M., Bautz M., et al., 1981, ApJ, 246, 951
Chakrabarty D., Grunsfeld J., Prince T.A., et al., 1993, ApJ, 403, L33
Dal Fiume D., Orlandini M., Cusumano G., et al., 1998, A&A, 329, L41
Dal Fiume D., Orlandini M., Del Sordo S., et al., 1999, ASR, in press (astro-ph/9906086)
Frontera F., Costa E., Dal Fiume D., et al., 1997, A&AS, 122, 357
Grove J.E., Strickman M., Johnson W.N., et al., 1995, ApJ, 438, L25
Kamata Y., Koyama K., Tawara Y., et al., 1990, PASJ, 42, 785
Makishima K., Mihara T., 1992, in Frontiers of X–ray Astronomy, eds. Tanaka Y., Koyama K. Universal Academy Press, Tokyo, 23
Manzo G., Giarrusso S., Santangelo A., et al., 1997, A&AS, 122, 341
Mészáros, P. 1992, High-Energy Radiation from Magnetized Neutron Stars, Chicago Univ. Press
Mihara T., 1995, PhD thesis, RIKEN
Orlandini M., Dal Fiume D., Frontera F., et al., 1998a, A&A, 332, 121
Orlandini M., Dal Fiume D., Frontera F., et al., 1998b, ApJ, 500, L163
Parmar A.N., Branduardi-Raymont G., Pollard G.S.G., et al., 1980, MNRAS, 193, 49P
Parmar A.N., Martin D., Bavdaz M., et al., 1997, A&AS, 122, 309
Polidan R.S., Pollard G.S., Sanford P.N., et al., 1978, Nat, 275, 296
Soong Y., Gruber D.E., Peterson L.E., et al., 1990, ApJ, 348, 641
Tanaka Y., 1986, in Radiation Hydrodynamics in Stars and Compact Objects, eds. Mihalas D., Winkler K.H. Springer, Berlin, 198
Valinia A., Marshall F.E., 1998, ApJ, 505, 134
White N.E., Pravdo S.H., 1979, ApJ, 233, L121
White N.E., Swank J.H., Holt S.S., 1983, ApJ, 270, 711